Full-car active suspension based on $\mathcal{H}_2$/generalised $\mathcal{H}_2$ output feedback control

Shuyou Yu

State Key Laboratory of Automotive Simulation and Control,
Department of Control Science and Engineering,
Jilin University,
Mailbox # 9, Nanhu Campus, Nanhu Road #5372,
Changchun 130012, China
Email: shuyou@jlu.edu.cn

Fei Wang

Department of Control Science and Engineering,
Jilin University,
Room 520, Laboratory Building,
Nanling Campus, Changchun 130025, China
Email: ttian_faye_2010@163.com

Jing Wang

Department of Control Science and Engineering,
Jilin University, China,
Mailbox #9, Nanhu Campus,
Nanhu Road #5372, Changchun 130012, China
Email: jean_hardworking@163.com

Hong Chen*

State Key Laboratory of Automotive Simulation and Control,
Department of Control Science and Engineering,
Jilin University, China,
Room 427, Laboratory Building,
Nanling Campus, Changchun 130025, China
E-mail: chenh@jlu.edu.cn
*Corresponding author

Abstract: This paper establishes a 15 degree-of-freedom (DOF) full-car simulation model for the car Hongqi HQ3. The effectiveness of the model is evaluated by comparison of the real data of HQ3 with the data of the model. Output feedback control of the active suspension is designed based on a half-car model. High quality ride comfort is achieved by minimising the $\mathcal{H}_2$ norm from disturbances on the road to the vertical acceleration and the pitch

acceleration of the car, while safety constraints such as suspension dynamic travels, static/dynamic load ratios and normalised load flows are guaranteed by the generalised $\mathcal{H}_2$ norm. The 15 DOF full-car model, together with the left and the right output feedback controllers, form a closed-loop system. The simulation result of the full-car shows that the active suspension can greatly reduce the vertical acceleration, pitch acceleration and roll acceleration as well as satisfy all constraints.

Keywords: full-car simulation model; active suspension; $\mathcal{H}_2$/generalised $\mathcal{H}_2$ control; output feedback control.

Biographical notes: Shuyou Yu has been an Associate Professor with Department of Control Science and Engineering at the Jilin University, China, since March 2012. He received his BS and MS in Control Science and Engineering at Jilin University, China, in 1997 and 2005, respectively, and PhD in Engineering Cybernetics at the University of Stuttgart, Germany, in 2011. From 2010 to 2011, he was a research and teaching assistant at the Institute for Systems Theory and Automatic Control at the University of Stuttgart. His main areas of interest are in model predictive control, robust control, and applications in mechatronic systems.

Fei Wang received the BS from Jilin University, Changchun, China, in 2010, where she is currently working toward the PhD degree in Control Theory and Control Engineering. Her current research interests include nonlinear systems control, model predictive control, robust control, vehicle stability control after tire blow-out and fast realisation of algorithm with field programmable gate array.

Jing Wang received the BS in Control Science and Engineering at the Jilin University, China, in 2013. She is currently studying for a Master's degree in Control Science and Engineering at the Jilin University. Her research interests include robust control, active suspension control and active four-wheel steering control.

Hong Chen received the BS and MS in Process Control from Zhejiang University, Zhejiang, China, in 1983 and 1986, respectively, and the PhD from the University of Stuttgart, Stuttgart, Germany, in 1997. In 1986, she joined Jilin University of Technology, Changchun, China. From 1993 to 1997, she was a wissenschaftlicher Mitarbeiter at the Institut fuer Systemdynamik und Regelungstechnik, University of Stuttgart. Since 1999, she has been a Professor with Jilin University, where she is presently a Tang Aoqing Professor. Her current research interests include model predictive control, optimal and robust control, nonlinear control, and applications in process engineering and mechatronic systems.

1 Introduction

The suspension system is an essential element of the vehicle which passes all the force and torque from the wheels to the sprung mass. The design of advanced suspension systems is influenced by several conflicting performance requirements:

- isolating passengers from vibration and shock arising from road roughness (ride comfort)

- suppressing the hop of the wheels so as to maintain firm and uninterrupted contact of wheels to road (good road holding or good handling)

- keeping suspension strokes within an allowable maximum (Hrovat, 1997; Chen and Guo, 2005).

That is, the conflicting tasks of providing excellent ride comfort and ride safety, while simultaneously meeting constructional constraints, have to be resolved.

To manage the tradeoff between the conflicting performance requirements, many active suspension control approaches are proposed such as LQG (Gordon et al., 1991; Ulsoy et al., 1994), sliding mode control (Kurimoto and Yoshimura, 1998; Li et al., 2009), backstepping control (Lin and Huang, 2003), adaptive control (Alleyne and Hedrick, 1995; Fialho and Balas, 2010; Sun et al., 2015), predictive control (Kashtiban et al., 2009) and preview control (Li and Liu, 2009). $\mathcal{H}_\infty$ active suspensions are discussed in the context of robustness and disturbance attenuation (Du and Zhang, 2007; Yamashita et al., 1994; Park et al., 1999; Karlsson et al., 2001; Hayakawa et al., 1999; Fialho and Balas, 2010), where all requirements, including those associated with hard constraints, are weighted and formulated in a single objective functional. On one hand, specifying all different requirements in a single objective functional may lead to conservativeness. On the other hand, choosing appropriately frequency-dependent weights to manage the tradeoff between conflicting requirements is not a trivial work. Active suspension control problems are formulated as a disturbance attenuation problem with hard time-domain constraints (Chen and Guo, 2005; Ma and Chen, 2011), where $\mathcal{H}_\infty$ performance is used to measure ride comfort. The problem formulation benefits ride comfort, respecting the safety relevant constraints at the same time, and can be implemented easily, since it has only one adjustable parameter. Since not all the states of the active suspension are available, the static $\mathcal{H}_\infty$ output feedback controller for vehicle suspension is exploited in Yu et al. (2006) and Du and Zhang (2008).

In the context of vehicle ride and handling, road disturbances can be generally classified as shock and vibration (Hrovat, 1997; Chen and Guo, 2005). Shocks are discrete events of relatively short duration and high intensity, caused by, for example, a pronounced bump or pothole on an otherwise smooth road. Vibrations, on the other hand, are consistent and typically specified as a random process with a ground displacement power spectral density. Thus, the ground velocity can be viewed as a white noise with impulse. Rather than $\mathcal{H}_\infty$ norm, $\mathcal{H}_2$ norm is appropriate to describe the road unevenness, since the squared $\mathcal{H}_2$ norm of the systems coincides with the total 'output energy' of the system when the disturbance is impulse input signals. Also it is appropriate because it accords with the asymptotic output variance of the system when it is excited by white noise input signals (Scherer and Weiland, 2000). Generalised $\mathcal{H}_2$ (also named energy-bounded-peak) control and estimation is widely discussed (Yu et al., 2006; Du and Zhang, 2008, 2010; Zhang et al., 2012, 2014a,b), and is normally used to constrain hard limitations. Hence, $\mathcal{H}_2$/generalised $\mathcal{H}_2$ output feedback control is selected as the control strategy of the active suspension in Chen et al. (2007), where

$\mathcal{H}_2$ performance is used to improve ride comfort and generalised $\mathcal{H}_2$ is used to deal with safety constraints. A quarter vehicle or a half vehicle suspension model rather than a full-car vehicle dynamic model is used as as a simulation model in Chen and Guo (2005), Chen et al. (2007), Li and Liu (2009), Du and Zhang (2010) and Ma and Chen (2011), where the simulation model is the same as the model used as a designing controller. Thus, the complex vehicle dynamic is not fully taken into account. In this paper, firstly, a 15 degree-of-freedom (DOF) full-car simulation model is established in the multi-body dynamics software – advanced modelling environment for simulation of engineering systems (AMESim), which will be used to verify the effectiveness of the proposed active suspension system. Then, $\mathcal{H}_2$/generalised $\mathcal{H}_2$ output feedback control algorithm is exploited, and $\mathcal{H}_2$/generalised $\mathcal{H}_2$ output feedback controllers of half-car suspension are developed. The controller based on a half-car model is much simpler to implement since the order of it is much smaller than the controller based on the full-car model. The closed-loop system is established by connecting the 15 DOF full-car model with the left and the right output feedback controllers. A simulation experiment is carried out in which the vehicle was driven on the road with convex hull at a uniform speed. The simulation results show that the proposed active suspension can greatly improve the handling stability and ride comfort of the vehicle as well as safety constraints. Note that this paper does not aim to propose a new control scheme, but to offer a blueprint for the solution of the full-car active suspension control problem using the existing control scheme. The blueprint is evaluated by a vehicle dynamic simulation experiment in AMESim, and the controller has a lower order than the plant.

This paper is organised as follows. In Section 2, a 15 DOF full-car simulation model is designed in AMESim software. In Section 3, firstly, a four DOF half-car model and control problem are discussed. Then, $\mathcal{H}_2$/generalised $\mathcal{H}_2$ output feedback control and controller design are exploited, respectively. In Section 4, a simulation test is implemented where the vehicle was driven on the road with a convex hull. A short summary is given in Section 5.

2 Full-car simulation model

Full-car modelling based on traditional mathematical methods is difficult to guarantee the accuracy of the model. The theory of multi-body dynamics and its softwares provide a powerful tool for the full-car modelling and simulation. Multi-body dynamic system is composed of multiple objects, such as rigid body, flexible body, soft body, particle, etc, which are connected together through a variety of constraints. Multi-body dynamics contain the classical rigid body mechanics, analytical mechanics, computer simulation technology and so on. In this paper, a 15 DOF full-car model is established in AMESim, one of multi-body dynamics softwares. The model is used as the plant of active suspension systems. The construction of the vehicle model is displayed in Figure 1, which is composed of several sub-systems, such as chassis, suspension, steering system, driveline and brake system, road, tyre, etc. The parameters of the vehicle model are from the car of Hongqi HQ3 which is produced by the first automobile works (FAW) in China. Some parameters are given in Table 1.

The automotive chassis provides the strength necessary to support the vehicular components and the payload placed upon it. The suspension system contains the springs, the shock absorbers, and other components that allow the vehicle to be driven on uneven terrain (Chen, 2005). The suspension stiffness and damping determine the vehicle's handling stability and ride comfort. The anti-roll bar can reduce the roll movement of the vehicle.

The steering mechanism is an integral portion of the chassis, and it provides the operator to control the direction of travel. The body of the vehicle encloses the mechanical components which make up the chassis and are held together in proper relation to each other by the frame. The steering system, the drive-line system and the brake system are designed, which permit the vehicle to track a given velocity and steering angle. Four reference frames like galilean frame, car body frame, spindle frame and wheel frame are established.

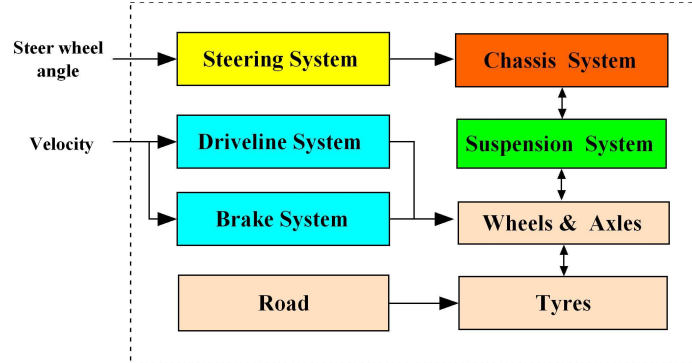**Figure 1** Vehicle model in AMESim (see online version for colours)
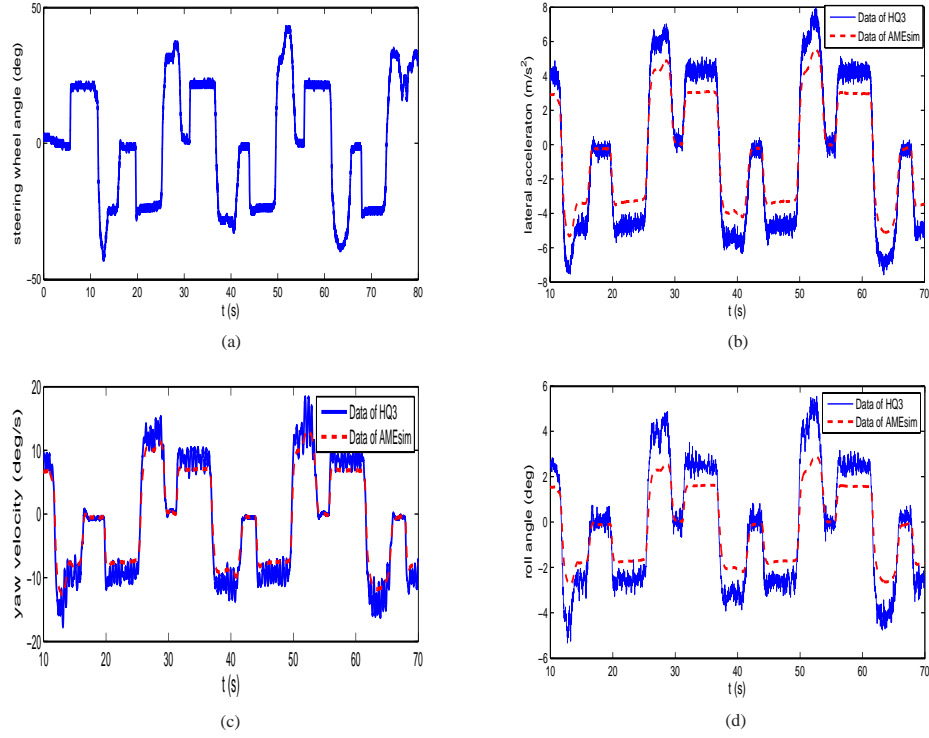

Table 1 Vehicle dynamic parameters

Parameters	Value
Sprung mass (m_s)	1632 kg
Pitch inertia (I_φ)	2770 kg·m^2
Front un-sprung mass for single wheel (m_{u1})	46.6 kg
Rear un-sprung mass for single wheel(m_{u2})	49.2 kg
Front suspension stiffness (k_{s1})	27,450 N/m
Rear suspension stiffness (k_{s2})	35,550 N/m
Front suspension damping (c_{s1})	3023 N·s/m
Rear suspension damping (c_{s2})	2894 N·s/m
Front tyre stiffness (k_{t1})	249,315 N/m
Rear tyre stiffness (k_{t2})	249,315 N/m
Distance between centre of gravity and front axle (l_f)	1.368 m
Distance between centre of gravity and rear axle (l_r)	1.482 m
Track distance (L)	1.535 m

The tyre model used in this paper is the Magic tyre formula which has been widely used in the automotive field. The Magic tyre formula defines the longitudinal force F_x, the lateral force F_y and the aligning torque M_z with only one formula (Pacejka, 1973; Pacejka and Besselink, 1997). The road model is very important in the vehicle dynamics simulation, since a better road model can make the simulation result more effective (James, 2000). In this paper we consider the flat road with a convex hull.

To verify and validate the full-car model, a comparison of the vehicle dynamics is utilised which have the same velocity and steering wheel angle between the full-car model and the data of the real car HQ3. Figures 2 and 3 show the plots of lateral acceleration, yaw velocity

and roll angle of the steering wheel angle step input and impulse input, respectively. Both curve shapes and peak values show the good correlation and consistency.

Figure 2   Simulation analysis of steering wheel angle step input. Solid line: data of HQ3, dashed line: full-car model: (a) steering wheel angle; (b) lateral acceleration; (c) yaw velocity and (d) roll angle (see online version for colours)
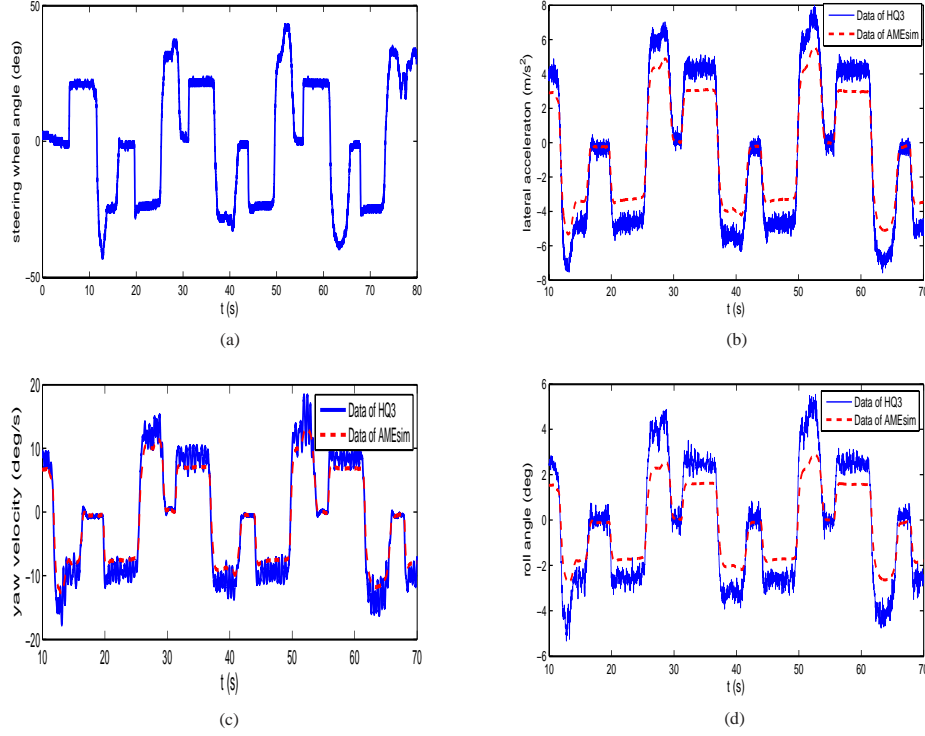

Remark 1:   To simplify the model and reflect the performance concerned, some factors such as the dynamics of the two front wheels, the influence of air resistance and wind are ignored in the process modelling. The factors may cause the deviations between the data obtained from HQ3 and those of the full car model.

3   Active suspension design

In this section, control of half-car active suspensions based on the $\mathcal{H}_2$/generalised $\mathcal{H}_2$ output feedback control scheme is discussed. Firstly, the scheme of $\mathcal{H}_2$ / generalised $\mathcal{H}_2$ output feedback control is introduced, where the corresponding optimisation problem is a convex optimisation problem involving linear matrix inequalities (LMIs) (Chen et al., 2003; Scherer et al., 1997). Then, a four DOF half-car model is described and control requirements for the active suspension are discussed. Finally, the suggested output feedback control approach is used to design active suspensions based on the four DOF half-car model.

Figure 3 Simulation analysis of steering wheel angle impulse input. Solid line: data of HQ3, dashed line: full-car model: (a) steering wheel angle; (b) lateral acceleration; (c) yaw velocity and (d) roll angle (see online version for colours)

3.1 $\mathcal{H}_2$/generalised $\mathcal{H}_2$ output feedback control

Consider linear time-invariant (LTI) systems

$$\begin{cases} \dot{x}(t) = Ax(t) + B_w w(t) + B_u u(t) \\ z_1(t) = C_1 x(t) + D_1 w(t) + D_{1u} u(t) \\ z_2(t) = C_2 x(t) + D_2 w(t) + D_{2u} u(t) \\ y(t) = C_y x(t) + D_{yw} w(t) \end{cases} \tag{1}$$

where $x \in R^{n_x}$ is the system states, $u \in R^{n_u}$ the control inputs, $w \in R^{n_w}$ the exogenous inputs (such as disturbance signals and sensor noise), $z_1 \in R^{n_{z1}}$ the outputs related to the performance of the system, $z_2 \in R^{n_{z2}}$ the outputs related to the constraint conditions of the system, and $y \in R^{n_y}$ the feedback outputs.

Consider an output feedback controller

$$\begin{cases} \dot{\zeta}(t) = A_K \zeta(t) + B_K y(t) \\ u(t) = C_K \zeta(t) + D_K y(t) \end{cases} \tag{2}$$

where $\zeta(t) \in R^{n_x}$. Denote $x_{cl} = \begin{bmatrix} x^T & \zeta^T \end{bmatrix}^T$, then the closed-loop systems are as follows:

$$\begin{cases} \dot{x}_{cl}(t) = A_{cl} x_{cl}(t) + B_{cl} w(t) \\ z_1(t) = C_{cl,1} x_{cl}(t) + D_{cl,1} w(t) \\ z_2(t) = C_{cl,2} x_{cl}(t) + D_{cl,2} w(t) \end{cases} \tag{3}$$

where

$$A_{cl} = \begin{bmatrix} A + B_u D_K C_y & B_u C_K \\ B_K C_y & A_K \end{bmatrix}$$

$$B_{cl} = \begin{bmatrix} B_w + B_u D_K D_{yw} \\ B_K D_{yw} \end{bmatrix}$$

$$C_{cl,1} = \begin{bmatrix} C_1 + D_{1u} D_K C_y & D_{1u} C_K \end{bmatrix}$$

$$C_{cl,2} = \begin{bmatrix} C_2 + D_{2u} D_K C_y & D_{2u} C_K \end{bmatrix}$$

$$D_{cl,1} = D_1 + D_{1u} D_K D_{yw}$$

$$D_{cl,2} = D_2 + D_{2u} D_K D_{yw}$$

The $\mathcal{H}_2$/generalised $\mathcal{H}_2$ output feedback control scheme is to find an output-feedback controller (2) such that the $\mathcal{H}_2$ norm from w to z_1 is minimised, and the generalised $\mathcal{H}_2$ norm from w to z_2 is less than ρ, where $\rho > 0$ is a given scalar.

Suppose there is a matrix $P \in R^{2n_x \times 2n_x}$ with $P > 0$. Partition P and P^{-1} as

$$P = \begin{bmatrix} Y & N \\ N^T & \star \end{bmatrix}, \; P^{-1} = \begin{bmatrix} X & M \\ M^T & \star \end{bmatrix}$$

with $YX + NM^T = I$ and $XY + MN^T = I$, where $\star$ is an unknown appropriate matrix, and $X, Y, M, N \in R^{n_x \times n_x}$. Define new variables

$$\hat{A} := N A_K M^T + N B_K C_y X + Y B_u C_K M^T$$
$$\qquad + Y(A + B_u D_K C_y)X$$
$$\hat{B} := N B_K + Y B_u D_K$$
$$\hat{C} := C_K M^T + D_K C_y X$$
$$\hat{D} := D_K.$$

An output feedback controller can be obtained by solving the following optimisation problem involving LMI constraints (Chen et al., 2003; Scherer et al., 1997)

Problem 1:

$$\underset{\nu, S, X, Y, \hat{A}, \hat{B}, \hat{C}, \hat{D}}{\text{minimise}} \quad \nu^2 \tag{4}$$

subject to

$$\begin{bmatrix} \mathfrak{A}_{11} & \mathfrak{A}_{12} & \mathfrak{A}_{13} \\ \circlearrowleft & \mathfrak{A}_{22} & \mathfrak{A}_{23} \\ \circlearrowleft & \circlearrowleft & -I \end{bmatrix} < 0,$$

$$\begin{bmatrix} X & \circlearrowleft & \circlearrowleft \\ I & Y & \circlearrowleft \\ C_1 X + D_{1u}\hat{C} & C_1 + D_{1u}\hat{D}C_y & S \end{bmatrix} > 0$$

$$D_1 + D_{1u}\hat{D}D_{yw} = 0$$

$$D_2 + D_{2u}\hat{D}D_{yw} = 0$$

$$\text{Trace}(S) < \nu^2, \tag{5}$$

where $\circlearrowleft$ denotes the symmetric part of a matrix and $\mathfrak{A}_{11} = AX + XA^T + B_u\hat{C} + (B_u\hat{C})^T, \mathfrak{A}_{12} = \hat{A}^T + (A + B_u\hat{D}C_y), \mathfrak{A}_{13} = B_w + B_u\hat{D}D_{yw}, \mathfrak{A}_{22} = A^TY + YA + \hat{B}C_y + (\hat{B}C_y)^T, \mathfrak{A}_{23} = YB_w + \hat{B}D_{yw}$.

Suppose that the optimisation Problem 1 has a solution $(\nu^*, S^*, X^*, Y^*, \hat{A}^*, \hat{B}^*, \hat{C}^*, \hat{D}^*)$, and there exist nonsingular matrixes M and N such that $MN^T = I - X^*Y^*$, then the output feedback control (2) is

$$
\begin{cases}
D_K := \hat{D}^*, \\
C_K := (\hat{C}^* - D_K C_y X^*)M^{-T}, \\
B_K := N^{-1}(\hat{B}^* - Y^* B_u D_K), \\
A_K := N^{-1}(\hat{A}^* - NB_K C_y X^* - Y^* B_u C_K M^T - Y^*(A + B_u D_K C_y)X^*)M^{-T},
\end{cases}
\tag{6}
$$

which guarantees that

- the closed loop system is internally stable

- the $\mathcal{H}_2$ norm from w to z_1 is minimised

- the generalised $\mathcal{H}_2$ norm from w to z_2 is bounded by the scalar ρ (Yu et al., 2006; Sun, 2004).

The proposed $\mathcal{H}_2$/generalised $\mathcal{H}_2$ output feedback controller has the same order as the physical plant, see equations (2) and (6). Generally, the simple linear controllers are normally preferred since they are easier to implement and have higher reliability than the complex linear controllers in system designs. Thus, a lower-order controller should be sought whenever the resulting performance degradation is kept within an acceptable level (Zhou et al., 1996).

The linearised dynamics of the full-car model is 18 orders (Smith and Wang, 2002). In this paper, lower-order controllers are directly designed based on the half-car model. The obtained controllers are connected with the full-car model in AMEsim, and the effectiveness of the closed-loop systems is tested in the next section.

3.2 Four DOF half-car model

Since the full-car model is symmetric, we decouple it into two half-car models, namely the bounce/pitch and roll/wrap half-cars (Smith and Wang, 2002; Ma and Chen, 2011). Figure 4 gives a schematic presentation of a half-car model, where (k_{s1}, c_{s1}) and (k_{s2}, c_{s2}) consist of the front and rear passive suspensions, k_{t1} and k_{t2} stand for the front and rear tire stiffness, m_{u1} and m_{u2} represent the front and rear unsprung masses, z_{s1} and z_{s2} are the front and rear displacement of the sprung masses, z_{u1} and z_{u2} are the front and rear displacement of the unsprung masses, $z_{s1} - z_{u1}$ and $z_{s2} - z_{u2}$ are the front and rear suspension strokes, $z_{u1} - z_{t1}$ and $z_{u2} - z_{t2}$ are the front and rear tire deflections, z_{t1} and z_{t2} are the front and rear vertical ground displacements caused by road unevenness. Moreover, m_s and I_θ are the vehicle mass and the pitch moment of inertia about the centre of mass, l_f and l_r are the front and rear distances from the centre of mass. Based on this half-car model, both heave and pitch modes in the sprung mass m_s are investigated, where z_c is the heave displacement and θ is the pitch angle. The linearised dynamic of the half-car vehicle dynamic is given

by equation (7), which has 4 DOF : the car body's vertical motion and pitch motion, the wheels' vertical motions (Yu, 2006; Gillespie, 1992).
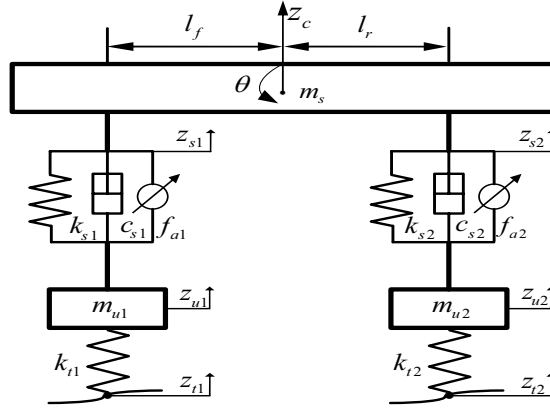
$$
\begin{cases}
m_s \ddot{z}_c = -c_{s1} (\dot{z}_{s1} - \dot{z}_{u1}) - c_{s2} (\dot{z}_{s2} - \dot{z}_{u2}) - k_{s1} (z_{s1} - z_{u1}) \\
\qquad - k_{s2} (z_{s2} - z_{u2}) + f_{a1} + f_{a2} \\
I_\theta \ddot{\theta} = l_f c_{s1} (\dot{z}_{s1} - \dot{z}_{u1}) - l_r c_{s2} (\dot{z}_{s2} - \dot{z}_{u2}) + l_f k_{s1} (z_{s1} - z_{u1}) \\
\qquad - l_r k_{s2} (z_{s2} - z_{u2}) - l_f f_{a1} + l_r f_{a2} \\
m_{u1} \ddot{z}_{u1} = k_{s1} (z_{s1} - z_{u1}) + c_{s1} (\dot{z}_{s1} - \dot{z}_{u1}) - k_{t1} (z_{u1} - z_{t1}) - f_{a1} \\
m_{u2} \ddot{z}_{u2} = k_{s2} (z_{s2} - z_{u2}) + c_{s2} (\dot{z}_{s2} - \dot{z}_{u2}) - k_{t2} (z_{u2} - z_{t2}) - f_{a2}.
\end{cases}
\tag{7}
$$

The normalised weighting function of the road profile is (Chen et al., 2003)

$$
\dot{z}_t = 2\pi n_0 \sqrt{G_0 V} w(t),
\tag{8}
$$

where $w(t)$ is a white noise whose mean value is 0 and power spectral density is 1, n_0 is the reference space frequency, G_0 is the road roughness coefficient, V is the velocity of the vehicle.

Figure 4   Structure of the half-car model

The active force f_{a1} and f_{a2} are, in general, generated by hydraulic actuators placed between the sprung and the unsprung masses (Ma and Chen, 2011). The model of the actuator is Alleyne and Hedrick (1995)

$$
\begin{cases}
f_a = A_r P_L \\
\dfrac{V_t}{4\beta_e} \dot{P}_L = Q_a - C_{tp} P_L - A_r (\dot{z}_s - \dot{z}_u),
\end{cases}
\tag{9}
$$

where f_a is the active force, A_r is the actuator ram area, P_L is the actual pressure, Q_a is the load flow, β_e is the effective bulk modulus, C_{tp} is the coefficient of total leakage owing to pressure, V_t is the total actuator volume.

The values of the half-vehicle model parameters used in the controller design were given in Table 2. Both the sprung mass m_s and the pitch inertia I_θ are half of the value in Section 2 of the full-car model according to Newton's laws of mechanics.

Table 2 Half-vehicle dynamics model parameters

Parameters	Values	Parameters	Values
m_s	816 kg	I_θ	1385 kg $\cdot$ m^2
m_{u1}	46.6 kg	m_{u2}	49.2 kg
l_f	1.368 m	l_r	1.482 m
c_{s1}	3023 N·s/m	c_{s2}	2894 N·s/m
k_{s1}	27,450 N/m	k_{s2}	35,550 N/m
k_{ti}	249,315 N/m	$S_{\max}$	0.08 m
Q_s	2×10^{-4} m^3 /s	P_s	1.03×10^7 Pa
$\frac{4\beta_e}{V_t}$	4.515×10^{13} N/m^5	αC_{tp}	1 s^{-1}
A_r	3.35×10^{-4}m^2		

3.3 Problem setup and controller design

The smaller the vertical acceleration and the pitch acceleration of the vehicles are, the higher quality ride quality is. Thus, to quantify ride comfort, the vertical acceleration and the pitch acceleration of the vehicles are chosen as the performance output

$$z_1 := \begin{bmatrix} \ddot{z}_c \\ \ddot{\theta} \end{bmatrix},$$

where $\begin{bmatrix} z_c \\ \theta \end{bmatrix} = \begin{bmatrix} 1 & -l_f \\ 1 & l_r \end{bmatrix}^{-1} \begin{bmatrix} z_{s1} \\ z_{s2} \end{bmatrix}$, cf. (Sun, 2004, Section 3.4).

Good handling requires a firm uninterrupted contact of wheels to road. That is, the dynamic tire loads should not exceed the static ones (Chen and Guo, 2005; Ma and Chen, 2011)

$$k_{ti}(z_{ui}(t) - z_{ti}(t)) \le f_{kti}, \quad i = 1, 2, \forall t \ge 0 \tag{10}$$

where g is the acceleration of gravity, and the static tire loads f_{kt1} and f_{kt2} are computed as follows

$$f_{kt1} = \frac{l_r m_s g + (l_f + l_r) m_{u1} g}{l_f + l_r}$$

$$f_{kt2} = \frac{l_f m_s g + (l_f + l_r) m_{u2} g}{l_f + l_r}$$

Moreover, the suspension stroke limitation

$$|z_{si}(t) - z_{ui}(t)| \le S_{\max}, \quad i = 1, 2, \forall t \ge 0 \tag{11}$$

has to be taken into account to prevent excessive suspension bottoming which will lead to rapid deterioration of the ride comfort and a possible structural damage. The load flow is bounded

$$|Q_{ai}(t)| \le Q_s, \quad i = 1, 2, \forall t \ge 0, \tag{12}$$

where Q_s is the bound of the load flow in terms of the bandwidth limits of the actuators (Ma and Chen, 2011). Clearly, equations (10)–(12) can be treated as time-domain hard

constraints. Thus, z_2 contains suspension dynamic travels, static/dynamic load ratios and normalised actuator pressures.

In summary, the active suspension control problem can be formulated as a constrained $\mathcal{H}_2$ control problem, i.e., find an output feedback controller such that $\mathcal{H}_2$ norm from w to the performance z_1 is minimised, while the time-domain hard constraints are satisfied arising from suspension dynamic travels, static/dynamic load ratios and normalised actuator pressures.

Define $x = \left[z_{s1} - z_{u1}, z_{s2} - z_{u2}, \dot{z}_{s1}, \dot{z}_{s2}, z_{u1} - z_{t1}, z_{u2} - z_{t2}, \dot{z}_{u1}, \dot{z}_{u2}, P_{L1}/P_s, \right.$ $\left. P_{L2}/P_s\right]^T$, $u = \left[\frac{Q_{a1}}{Q_s}, \frac{Q_{a2}}{Q_s}\right]^T$, and $w = [w_1, w_2]^T$, where P_s is the hydraulic supply pressure, then the active suspension system based on the half-car model can be written in the form of equation (1), where

$$A = \begin{bmatrix} A_{11} & A_{12} \\ A_{21} & A_{22} \end{bmatrix}^T, \quad C_1 = \begin{bmatrix} C_{11} & C_{12} \end{bmatrix}, \quad D_1 = D_{1u} = 0_{2\times 2}, \quad C_y = \begin{bmatrix} C_{31} & C_{32} \end{bmatrix},$$

$$A_{11} = \begin{bmatrix} 0 & 0 & -\frac{k_{s1}}{m_s} - \frac{k_{s1}l_f^2}{I_\theta} & -\frac{k_{s1}}{m_s} + \frac{k_{s1}l_f l_r}{I_\theta} \\ 0 & 0 & -\frac{k_{s2}}{m_s} + \frac{k_{s2}l_f l_r}{I_\theta} & -\frac{k_{s2}}{m_s} - \frac{k_{s2}l_r^2}{I_\theta} \\ 1 & 0 & -\frac{c_{s1}}{m_s} - \frac{c_{s1}l_f^2}{I_\theta} & -\frac{c_{s1}}{m_s} + \frac{c_{s1}l_f l_r}{I_\theta} \\ 0 & 1 & -\frac{c_{s2}}{m_s} + \frac{c_{s2}l_f l_r}{I_\theta} & -\frac{c_{s2}}{m_s} - \frac{c_{s2}l_r^2}{I_\theta} \\ 0 & 0 & 0 & 0 \end{bmatrix}, \quad A_{12} = \begin{bmatrix} 0 & 0 & \frac{k_{s1}}{m_{u1}} & 0 & 0 & 0 \\ 0 & 0 & 0 & \frac{k_{s2}}{m_{u2}} & 0 & 0 \\ 0 & 0 & \frac{c_{s1}}{m_{u1}} & 0 & -\frac{\alpha A_r}{P_s} & 0 \\ 0 & 0 & 0 & \frac{c_{s2}}{m_{u2}} & 0 & -\frac{\alpha A_r}{P_s} \\ 0 & 0 & -\frac{k_{t1}}{m_{u1}} & 0 & 0 & 0 \end{bmatrix},$$

$$A_{21} = \begin{bmatrix} 0 & 0 & 0 & 0 \\ -1 & 0 & \frac{c_{s1}}{m_s} + \frac{c_{s1}l_f^2}{I_\theta} & \frac{c_{s1}}{m_s} - \frac{c_{s1}l_f l_r}{I_\theta} \\ 0 & -1 & \frac{c_{s2}}{m_s} - \frac{c_{s2}l_f l_r}{I_\theta} & \frac{c_{s2}}{m_s} + \frac{c_{s2}l_r^2}{I_\theta} \\ 0 & 0 & A_r P_s\left(\frac{1}{m_s} + \frac{l_f^2}{I_\theta}\right) & A_r P_s\left(\frac{1}{m_s} - \frac{l_f l_r}{I_\theta}\right) \\ 0 & 0 & A_r P_s\left(\frac{1}{m_s} - \frac{l_f l_r}{I_\theta}\right) & A_r P_s\left(\frac{1}{m_s} + \frac{l_r^2}{I_\theta}\right) \end{bmatrix},$$

$$A_{22} = \begin{bmatrix} 0 & 0 & 0 & -\frac{k_{t2}}{m_{u2}} & 0 & 0 \\ 1 & 0 & -\frac{c_{s1}}{m_{u1}} & 0 & 0 & 0 \\ 0 & 1 & 0 & -\frac{c_{s2}}{m_{u2}} & 0 & 0 \\ 0 & 0 & -\frac{A_r P_s}{m_{u1}} & 0 & -\alpha C_{tp} & 0 \\ 0 & 0 & 0 & -\frac{A_r P_s}{m_{u2}} & 0 & -\alpha C_{tp} \end{bmatrix},$$

$$B_u = \begin{bmatrix} 0 & 0 & 0 & 0 & 0 & 0 & 0 & 0 & \frac{\alpha Q_s}{P_s} & 0 \\ 0 & 0 & 0 & 0 & 0 & 0 & 0 & 0 & 0 & \frac{\alpha Q_s}{P_s} \end{bmatrix}^T, \quad B_w = \begin{bmatrix} B_1 & B_2 \end{bmatrix}^T, \quad D_2 = D_{yw} = 0_{6\times 2},$$

$$B_1 = \begin{bmatrix} 0 & 0 & 0 & 0 & -2\pi n_0\sqrt{G_0 V} \\ 0 & 0 & 0 & 0 & 0 \end{bmatrix}, \quad B_2 = \begin{bmatrix} 0 & 0 & 0 & 0 & 0 \\ 0 & 0 & 0 & 0 & -2\pi n_0\sqrt{G_0 V} \end{bmatrix},$$

$$C_{11} = \begin{bmatrix} -\frac{k_{s1}}{m_s} & -\frac{k_{s2}}{m_s} & -\frac{c_{s1}}{m_s} & -\frac{c_{s2}}{m_s} & 0 \\ \frac{k_{s1}l_f}{I_\theta} & -\frac{k_{s2}l_r}{I_\theta} & \frac{c_{s1}l_f}{I_\theta} & -\frac{c_{s2}l_r}{I_\theta} & 0 \end{bmatrix}, \quad C_{12} = \begin{bmatrix} 0 & \frac{c_{s1}}{m_s} & \frac{c_{s2}}{m_s} & \frac{A_r P_s}{m_s} & \frac{A_r P_s}{m_s} \\ 0 & -\frac{c_{s1}l_f}{I_\theta} & \frac{c_{s2}l_r}{I_\theta} & -\frac{A_r P_s l_f}{I_\theta} & \frac{A_r P_s l_r}{I_\theta} \end{bmatrix},$$

$$C_2 = \begin{bmatrix} \frac{1}{S_{\max}} & 0 & 0 & 0 & 0 & 0 & 0 & 0 & 0 \\ 0 & \frac{1}{S_{\max}} & 0 & 0 & 0 & 0 & 0 & 0 & 0 \\ 0 & 0 & 0 & 0 & \frac{k_{t1}}{f_{kt1}} & 0 & 0 & 0 & 0 \\ 0 & 0 & 0 & 0 & 0 & \frac{k_{t2}}{f_{kt2}} & 0 & 0 & 0 \\ 0 & 0 & 0 & 0 & 0 & 0 & 0 & 0 & 0 \\ 0 & 0 & 0 & 0 & 0 & 0 & 0 & 0 & 0 \end{bmatrix}, \quad C_{31} = \begin{bmatrix} -\frac{k_{sf}}{m_s} & -\frac{k_{sr}}{m_s} & -\frac{c_{sf}}{m_s} & -\frac{c_{sr}}{m_s} & 0 \\ \frac{k_{sf}l_f}{I_\theta} & -\frac{k_{sr}l_r}{I_\theta} & \frac{c_{sf}l_f}{I_\theta} & -\frac{c_{sr}l_r}{I_\theta} & 0 \\ 1 & 0 & 0 & 0 & 0 \\ 0 & 1 & 0 & 0 & 0 \\ 0 & 0 & 0 & 0 & 0 \\ 0 & 0 & 0 & 0 & 0 \end{bmatrix},$$

$$C_{32} = \begin{bmatrix} 0 & \frac{c_{sf}}{m_s} & \frac{c_{sr}}{m_s} & \frac{A_r P_s}{m_s} & \frac{A_r P_s}{m_s} \\ 0 & -\frac{c_{sf} l_f}{I_\theta} & \frac{c_{sr} l_r}{I_\theta} & -\frac{A_r P_s l_f}{I_\theta} & \frac{A_r P_s l_r}{I_\theta} \\ 0 & 0 & 0 & 0 & 0 \\ 0 & 0 & 0 & 0 & 0 \\ 0 & 0 & 0 & 1 & 0 \\ 0 & 0 & 0 & 0 & 1 \end{bmatrix}, \quad D_{2u} = \begin{bmatrix} 0\,0\,0\,0\,1\,0 \\ 0\,0\,0\,0\,0\,1 \end{bmatrix}^T .$$

Assume that the vertical acceleration and the body pitch acceleration $(\ddot{z}_c, \ddot{\theta})$, suspension dynamic travels $z_{si} - z_{ui}$ and normalised actuator pressures P_{Li}/P_s, $i = 1, 2$, can be measured, then the measured output y contains vertical acceleration, suspension dynamic travels and normalised actuator pressures, i.e.,

$$y = \begin{bmatrix} \ddot{z}_c\ \ddot{\theta}\ z_{s1} - z_{u1}\ z_{s2} - z_{u2}\ P_{L1}/P_s\ P_{L2}/P_s \end{bmatrix}^T .$$
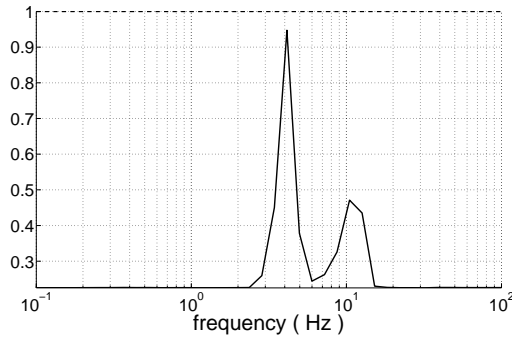
An output feedback control law (6) is obtained by solving the convex optimisation problem involving LMI which minimises $\mathcal{H}_2$ norm from w to z_1 as well as guarantees that generalised $\mathcal{H}_2$ norm from w to z_2 is less than ρ. Therefore, the ride comfort of the vehicle is improved and all the safety constraints are satisfied with respect to disturbances of the road.

Remark 2: The active force $f_a = A_r P_L$ where P_L is a function of the load flow Q_a, cf. equation (9). Since the load flow is bounded, cf. equation (12), the actuator saturation is considered.

3.4 Robust analysis

μ analysis is an useful tool to analyse and quantify the robustness of feedback control systems with respect to model perturbations and structured uncertainties (Zhou et al., 1996). Suppose that the sprung mass m_s and the pitch inertia I_θ have $\pm 25\%$ variation, and the front and rear tyre stiffness $k_{ti}(i = 1, 2)$ have $\pm 10\%$ variation. The μ curve of the active suspension system of the half-car model is given in Figure 5. It is shown that the system is robustly stable with respect to the given parameter perturbations since $\mu < 1$ for all frequencies.

Figure 5 μ analysis of half-car active suspension

Note that the robust stability of half-car active suspension systems do not mean the robust stability of the full-car active suspension system. Moreover, if the half-car active suspension

system is non-robustness with respect to the given model perturbations and structured uncertainties, the full-car active suspension system is non-robust neither since the left-right symmetry assumption is made in Section 3.2.
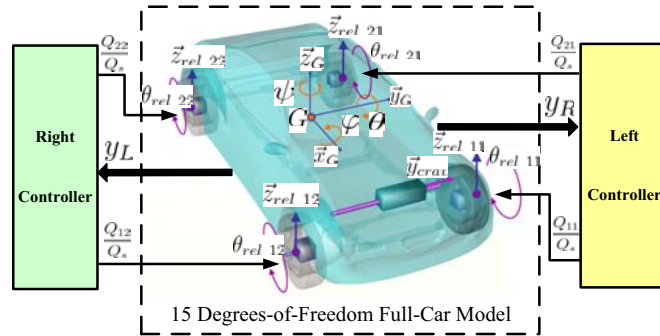
4   Closed-loop testing

In this section, the active suspension based on the $\mathcal{H}_2$/generalised $\mathcal{H}_2$ output feedback control strategy is connected with the 15 DOF full-car model in AMESim software, which form a closed-loop system, see Figure 6. There are two controllers where the left controller is related to the left half-car, and the right controller is related to the right half-car, respectively. The unilateral car body vertical accelerations are defined:

$$\begin{cases} \ddot{z}_{cL} = \ddot{z}_G + \ddot{\varphi}L\cos(\varphi)/2 \\ \ddot{z}_{cR} = \ddot{z}_G - \ddot{\varphi}L\cos(\varphi)/2 \end{cases} \tag{13}$$

where $\ddot{z}_G$ is the vertical acceleration of car body centre of gravity, φ is the roll angle, L the track distance, z_{cL} and z_{cR} are the left and right vertical acceleration respectively.

One of the objectives of the controller is to make unilateral body vertical acceleration $(\ddot{z}_{cL}, \ddot{z}_{cR})$ and body pitch acceleration $\ddot{\theta}_G$ minimum, where $\ddot{\theta}_G = \frac{\ddot{\theta}_L + \ddot{\theta}_R}{2}$, and $\ddot{\theta}_L$ and $\ddot{\theta}_R$ are the left and right body pitch acceleration. So when the left road condition is the same with the right road condition, the vehicle has no roll motion ($\ddot{\varphi} = 0$, $\ddot{z}_{cL} = \ddot{z}_{cR} = \ddot{z}_G$), and both the left and right controller will cause $\ddot{z}_G$ and $\ddot{\theta}$ minimum; when the left road condition is different with the right road condition, the vehicle has roll motion ($\ddot{\varphi} \neq 0$, $\ddot{z}_{cL} \neq \ddot{z}_{cR}$). In this case, the left controller will keep $\ddot{z}_{cL}$ and $\ddot{\theta}$ small, and the right controller will keep $\ddot{z}_{cR}$ and $\ddot{\theta}$ small. Thus, $\ddot{z}_G$ is small since $\ddot{z}_G = (\ddot{z}_{cL} + \ddot{z}_{cR})/2$ obtained from (13). Because both $\ddot{z}_{cL}$ and $\ddot{z}_{cR}$ are minimum, the roll motion of the vehicle is restrained, and $\ddot{\varphi}$ is proper. That is to say, both the two controllers will make $\ddot{z}_G$, $\ddot{\varphi}$ and $\ddot{\theta}$ small while the left and right road conditions are different.

Figure 6   System integration: full-car model with $\mathcal{H}_2$/generalised $\mathcal{H}_2$ controllers for both the left and right active suspension sub-systems (see online version for colours)
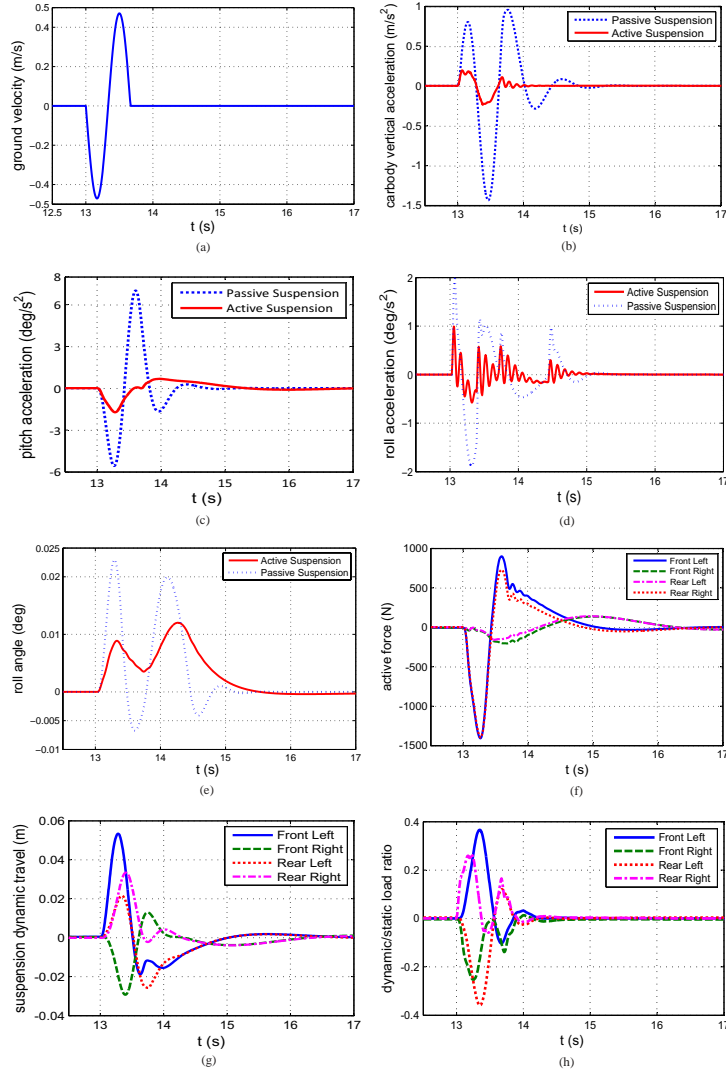

Consider the case of an isolated bump in an otherwise smooth road surface (Karlsson et al., 2001). The corresponding ground displacement is given by

$$z_t = \begin{cases} \frac{A}{2}\left(1 - \cos(\frac{2\pi V}{L}t)\right), & T < t < (T + \frac{L}{V}) \\ 0, & \text{Otherwise} \end{cases}$$

where A and L are the height and the length of the bump, $A = 10$ cm and $L = 10$ m, T is the time when the bump occurred. A vehicle dynamic simulation experiment is carried out to verify and validate the effect of the proposed controller. In the simulation, the vehicle left wheels pass a convex hull road with the speed of 15 m/s. The convex hull road can cause a severe vibration of the vehicle which will deteriorate the vehicle handling stability and ride comfort seriously. The response curves of the passive suspension and the active suspension are shown in Figure 7. The car body vertical acceleration, the pitch acceleration, and the roll acceleration of the vehicle with active suspension are significantly reduced, i.e., the vehicle ride comfort is significantly improved. Furthermore, the active forces, dynamic travels and static/dynamic load ratios of the active suspension do not exceed the boundaries.

Figure 7   Result of the simulation: (a) ground velocity; (b) car body vertical acceleration; (c) pitch acceleration; (d) roll acceleration; (e) roll angle; (f) active force; (g) suspension dynamic travel and (h) static/dynamic load ratio (see online version for colours)

5 Conclusions

A 15 DOF full-car model based on AMESim software was presented in this paper, and was validated and compared with the real car Hongqi HQ3 and used as the test platform of the vehicle active safety control.The higher precision nature of the simulation model renders it more practical. $\mathcal{H}_2$/generalised $\mathcal{H}_2$ output feedback controllers of half-car suspension was developed, and the closed-loop system was constructed by connecting the 15 DOF full-car model with the left and the right output feedback controllers. One of the most significant advantages of the proposed strategy is that the order of the controllers is much lower than the controllers based on the full-car model. A simulation experiment was carried out in which the vehicle drove on the road with a convex hull at a uniform speed. The simulation results showed that the proposed active suspension can greatly improve the handling stability, and meet the requirements for constraints satisfaction.

Acknowledgements

References

Alleyne, A. and Hedrick, J. (1995), 'Nonlinear adaptive control of active suspensions', *IEEE Trans. Contr. Syst. Technology*, Vol. 3, No. 1, pp.94–101.

Chen, J.R. (Eds.) (2005) *Automotive Structure*, China Mechine Press, Beijing.

Chen, H. and Guo, K-H. (2005) 'Constrained H$_\infty$ control of active suspensions: an LMI approach', *IEEE Contr. Syst. Tech.*, Vol. 13, No. 3, pp.412–421.

Chen, H., Sun, P-Y. and Guo, K-H. (2003) 'A multi-objective control design for active suspensions with hard constraints', *Proc. Amer. Contr. Conf.*, Colorado, USA, pp.4371–4376.

Chen, H., Ma, M-M. and Sun, P-Y. (2007) 'h_2/ generalized h_2 output feedback control for active suspension', *Control Theory and Applications*, Vol. 24, No. 5, pp.790–794.

Du, H.P. and Zhang, N. (2007) 'H_∞ control of ative vehicle suspensions with actuator time delay', *J. Sound Vib.*, Vol. 301, No. 1, pp.236–252.

Du, H.P. and Zhang, N. (2008) 'Designing H_∞/GH_2 static-output feedback controller for vehicle suspensions using linear marix inequalities', *Vehicle Systems Dynamics*, Vol. 46, No. 5, pp.385–412.

Du, H.P. and Zhang, N. (2010) 'Robust active suspension design subject to vehicle inertial parameter variations', *International Journal of Automation and Computing*, Vol. 7, No. 4, pp.419–427.

Fialho, I. and Balas, G.J. (2010) 'Design of nonlinear controllers for active vehicle suspensions using parameter-varying control synthesis', *Vehicle System Dynamics*, Vol. 33, No. 5, pp.351–370.

Gillespie, T. (1992) *Fundamentals of Vehicle Dynamics*, Society of Automotive Engineers, Warrendale.

Gordon, T.J., Marsh, C. and Milsted, M.G. (1991) 'A comparison of adaptive LQG and nonlinear controllers for vehicle suspension systems', *Vehicle System Dynamics*, Vol. 20, pp.321–340.

Hayakawa, K., Matsumoto, K., Yamashita, M., Suzuki, Y., Fujimori, K. and Kimura, H. (1999) 'Robust H_∞ output feedback control of decoupled automobile active suspension systems', *IEEE Trans. Automat. Contr.*, Vol. AC-44, pp.pp.392–396.

Hrovat, D. (1997) 'Survey of advanced suspension developments and related optimal control applications', *Automatica*, Vol. 33, No. 10, pp.1781–1817.

James, L. (2000) Tire model for simulations of vehicle motion on high and low friction road surfaces', *Proceedings of the 2000 Winter Simulation Conference*, pp.1025–1034.

Karlsson, N., Dahleh, M. and Hrovat, D. (2001) 'Nonlinear H_∞ control of active suspensions', *Proc. Amer. Contr. Conf.*, Arlington, VA, pp.3329–3334.

Kashtiban, A.M., Pourqurban, N., Alizadeh, G. and Hasanzadeh, I. (2009) 'Nonlinear optimal control of a half car active suspension', *2nd International Conference on Computer and Electrical Engineering*, pp.460–464.

Kurimoto, M. and Yoshimura, T. (1998) 'Active suspension of passenger cars using sliding mode controllers (based on reduced models)', *Int. J. Vehicle Design*, Vol. 19, No. 4, pp.402–414.

Li, X., Zheng, S., Zhang, J. and Li, K. (2009) 'Modelling and simulation study on application of sliding-mode control for an active anti-roll system in a passenger car with air suspension', *Int. J. Vehicle Design*, Vol. 49, No. 4, pp.318–337.

Li, Y. and Liu, S.J. (2009) 'Preview control of an active vehicle suspension system based on a four-degree-of-freedom half-car model', *Second International Conference on Intelligent Computation Technology and Automation*, pp.826–830.

Lin, J-S. and Huang, C-J. (2003) 'Nonlinear backstepping control design of half-car active suspension systems', *Int. J. of Vehicle Design*, Vol. 33, No. 4, pp.332–350.

Ma, M.M. and Chen, H. (2011) 'Disturbance attenuation control of active suspension with non-linear actuator dynamics', *IET Control Theory and Applications*, Vol. 5, No. 1, pp.112–122.

Pacejka, H.B. (1973) 'Simplified analysis of steady-state turning behaviour of motor vehicles', *Vehicle System Dynamics*, Vol. 2, No. 4, pp.161–172.

Pacejka, H.B. and Besselink, I. J.M. (1997) 'Magic formula tyre model with transient properties', *Vehicle System Dynamics*, Vol. 27, No. Supplement 001, pp.234–249.

Park, B.G., Lee, J.W. and Kwon, W.H. (1999) 'Robust one-step receding horizon control for constrained systems', *Int. J. Robust and Nonlinear Control*, Vol. 9, No. 7, pp.381–395.

Scherer, C., Gahinet, P. and Chilali, M. (1997) 'Multi-objective output-feedback control via LMI optimization', *IEEE Trans. Automat. Contr.*, Vol. 42, pp.896–911.

Scherer, C.W. and Weiland, S. (2000) *Linear Matrix Inequalities in Control*, DISC Lecture note, Dutch Institute of Systems and Control.

Smith, M.C. and Wang, F.C. (2002) 'Controller parameterization for disturbance response decoupling: application to vehicle active suspension control', *IEEE Trans. Auromat. Contr.*, Vol. 10, No. 3, pp.393–407.

Sun, P-Y. (2004) *Multi-Objective Control to Active Suspensions Based on LMI Optimization*, PhD Thesis, Jilin University, China.

Sun, W., Gao, H. and Kaynak, O. (2015) 'Vibration isolation for active suspensions with performance constraints and actuator saturation', *IEEE/ASME Transations on Mechatronics*, Vol. 20, pp.675–683.

Ulsoy, A., Hrovat, D. and Tseng, T. (1994) 'Stability robustness of LQ and LQG active suspensions', *ASME J. Dynamic Systems, Measurement, and Control*, Vol. 116, pp.123–131.

Yamashita, M., Fujimori, K., Hayakawa, K. and Kimura, H. (1994) 'Application of H_∞ control to active suspension systems', *Automatica*, Vol. 30, No. 11, pp.1717–1729.

Yu, Z. (2006) *Automotive Theory*, China Machine Press, Beijing.

Yu, S., Ma, M. and Chen, H. (2006) 'H_∞/ generalized H_2 output-feedback active suspension control via LMI optimization', *Journal of Nanjing University of Aeronautics and Astronautics*, Vol. 38, No. Supplement 1, pp.25–29.

Zhang, H., Shi, Y. and Cui, H. (2012) *Observer-Based Tracking Controller Design for Networked Predictive Control Systems with Uncertain Markov Delays*, Fairmont Queen Elizabeth, Montreal, Canada, pp.5682–5687.

Zhang, H., Shi, Y. and Wang, J. (2014a) 'On energy-to-peak filtering for nonuniformly sampled nonlinear systems: a Markovian jump system approach', *IEEE Transactions on Fuzzy Systems*, Vol. 22, No. 1, pp.212–222.

Zhang, H., Zhang, X. and Wang, J. (2014b) 'Robust gain-scheduling energy-to-peak control of vehicle lateral dynamics stabilizing', *Vehicle System Dynamics*, Vol. 52, No. 3, pp.309–340.

Zhou, K., Doyle, J.C. and Glover, K. (1996) *Robust and Optimal Control*, Prentice-Hall, Upper Saddle River, New Jersey.